



Efficiency and fuel utilization of methane-powered single-chamber solid oxide fuel cells

Yong Hao*, David G. Goodwin

Division of Engineering and Applied Science, California Institute of Technology, Pasadena, CA 91125, USA

ARTICLE INFO

Article history:

Received 7 March 2008

Received in revised form 25 April 2008

Accepted 28 April 2008

Available online 4 May 2008

Keywords:

Single-chamber fuel cell

Methane

Efficiency

Fuel utilization

ABSTRACT

The single-chamber solid oxide fuel cell (SC-SOFC) is a simplification of the conventional dual-chamber SOFC and has great potential for meeting portable power generation needs. While the high energy density of hydrocarbon fuels makes SC-SOFC a promising candidate as a power source for scenarios where portability is most preferred, the low efficiency and fuel utilization reported by many experimental groups have presented a major barrier keeping it from real application.

Based on an experimentally validated numerical model, this work systematically investigates the fuel cell efficiency and fuel utilization of a methane-powered SC-SOFC as a function of operating parameters including flow rate, fuel-to-oxygen ratio, fuel cell layout and balance gas. We predict that the maximum achievable efficiency of a single-cell SC-SOFC is above 10% and the efficiency at typical operating conditions is above 5%, significantly higher than the reported 1% in literature. Optimization approaches are proposed at different levels in terms of both improving the power output and reducing the unspent fuel.

© 2008 Elsevier B.V. All rights reserved.

1. Introduction

Single-chamber solid oxide fuel cells (SC-SOFCs) have attracted considerable attention in recent years as they have demonstrated progressively higher energy densities for portable power applications and the potential to reduce SOFC costs. Significant progress has been achieved experimentally in both enhancing the power density and reducing the operating temperature by way of doping noble metals in the anode and using higher hydrocarbons as the fuel [1]. In addition, the exothermic reactions incurred by the mixing of fuel and air lead to a significant temperature increase, not only reducing the ohmic resistance of the electrolyte but also making thermally self-sustained SC-SOFC possible [1,2].

Despite these attractions for portable power generation of SC-SOFCs, the thermal efficiency and fuel utilization remain very low. At this time, the reported thermal efficiency is about 1% [2], and the fuel utilization efficiency is less than 4% [3]. Compared with dual-chamber SOFCs, the low efficiencies of SC-SOFCs are primarily due to the inherently different flow geometry in which not only half of the fuel passes through the cathode side unreacted, but also the residence time of the flow over the cell is much shorter. In addition, while the usage of large amounts

of balance gas in order to prevent explosions in the gas mixture is necessary, it dilutes the fuel stream at the same time and thus lowers the performance. In the experimental studies reported so far, a significant portion utilized un-optimized gas chamber designs and fixed flow rates. Most of these studies tested a single cell instead of a cell stack. Although these test conditions helped to improve single-cell performance and eased both measurement and analysis, they were also, undoubtedly, the major barriers to higher fuel cell efficiencies; keeping SC-SOFCs just a laboratory curio, insufficient to satisfy real application needs.

Among the reported studies (both experimental and theoretical) about SC-SOFCs, most were carried out with lower hydrocarbon fuel, especially methane. There are several reasons for the preference of methane fuel. First, the catalytic reactions of methane are simpler and more studied as compared to the catalytic reactions of higher hydrocarbons; second, the relatively high operating temperature (above 550 °C [4]) for methane-powered cells is beneficial for both chemical kinetics in the electrodes and the reduction of ohmic resistance in the electrolyte; third, methane has a lower propensity for coking; lastly, from an economic point of view, methane is the most abundant hydrocarbon in nature and is widely available at low costs for real applications. The design issues with regard to fuel cell efficiency in this work are also explored with methane fuel in keeping with our previous studies [5,6]. To avoid repetition with experimental literature, this work lays more emphasis on areas that are less frequently explored experimentally, including

* Corresponding author. Tel.: +1 626 395 1711; fax: +1 626 385 8868.

E-mail address: haoyong@caltech.edu (Y. Hao).

flow geometry design, flow rate control and fuel/oxygen ratio, for the improvement of fuel cell efficiencies.

2. Efficiencies of the SC-SOFC

For a fuel cell system in general, the thermal efficiency (or efficiency) is defined as the ratio of the electric power and the total heat release associated with the full oxidation of the inlet fuel [7]:

$$\varepsilon = \frac{W_e}{Q_{in}} = \frac{\int i E_{cell} dA}{\dot{m}_{f,in} \Delta h_{f,in}} \quad (1)$$

where the electric power W_e is obtained by integrating the current density i along the effective cell area, multiplied by the load potential E_{cell} , and the total heat release Q_{in} of the fuel involves the total mass flow rate $\dot{m}_{f,in}$ and the combustion enthalpy change $\Delta h_{f,in}$ specifying low or high heat values for the fuel at the inlet.

The fuel utilization (efficiency), on the other hand, is defined as the ratio of the total enthalpy drop of the fuel (assuming full oxidation of any available fuels) between the inlet and the outlet to the total heat release Q_{in} of the inlet fuel:

$$\varepsilon_U = 1 - \frac{\dot{m}_{f,out} \Delta h_{f,out}}{\dot{m}_{f,in} \Delta h_{f,in}} \quad (2)$$

Fuel utilization ε_U is related to the fuel cell efficiency ε by

$$\varepsilon = \varepsilon_R \varepsilon_V \varepsilon_U \quad (3)$$

in which the reversible efficiency ε_R and the voltage or part-load efficiency ε_V are, respectively, defined by

$$\varepsilon_R = \frac{\Delta G}{\Delta H} = 1 - T \frac{\Delta S}{\Delta H} \quad (4)$$

$$\varepsilon_V = \frac{E_{cell}}{E_{rev}} \quad (5)$$

where ΔG , ΔH and ΔS are the changes in molar free energy, enthalpy and entropy, respectively, while E_{cell} and E_{rev} are the operating cell potential and Nernst potential, respectively. Since the definitions of efficiency and fuel utilization consider only the fuel but not oxygen, they apply equally well to dual- and single-chamber SOFCs.

For SC-SOFCs in particular, the experimental literature tends to use current efficiency to represent the fuel utilization [3,8,9]. The current efficiency is defined as the ratio of the actual current density i of the cell and the current density calculated for full fuel conversion i_F [10]:

$$\varepsilon_i = \frac{i}{i_F} \quad (6)$$

where, for a methane-powered cell, i_F is determined by Faraday's law, the gas flow rate, and the following equations [8,10]:



In practice, the current efficiency is calculated using the total current I of the cell and the total converted current I_F instead of the corresponding current densities, since the latter vary with location within the cell. Although it is intuitive that I_F scales with the inlet fuel amount and that I relates to the difference of the total energy of the fuel between the inlet and outlet from an energy conservation perspective, the current efficiency is insufficient compared to fuel utilization in several ways.

1. In the definition of current efficiency, the partial oxidation reaction of methane is only an assumption, but this assumption is unreasonable [11]. We identified a general three-layer structure for catalytic reactions within the fuel cell anode, and the amount of hydrogen and CO actually produced as well as the global reaction all sensitively depend on many design parameters and operating conditions. As a result, the definition of i_F is not specific, not accurate and only makes sense formally.

2. The current efficiency considers only the electric power output W_e on the external load, since

$$\varepsilon_i = \frac{I}{I_F} = \frac{IU}{I_F U} = \frac{W_e}{I_F U} \quad (10)$$

where U is the load potential. The definition of fuel utilization involves both W_e and other heating effects such as the charge-transfer heating at the electrode–electrolyte interfaces and the ohmic heating within the electrolyte.

3. The definition of fuel utilization involves any possible heat release associated with burning the available fuels, but that of current density completely neglects the heat effects and considers only the Faradaic conversion from fuel to current. For example, in the case with one mole of methane as the inlet fuel, then at a typical SC-SOFC operating temperature of 750 °C, the total heat release for fully oxidizing the methane is $Q_{in} = 803$ kJ. However, the total amount of electrons generated by the fuel can be calculated as $n = 6F$. Since SOFCs achieve their peak power density at or below $U = 0.8$ V [7], the electrons correspond to a total energy of no more than $nU = 463$ kJ, much lower than the combustion heat. As a result, for the same cell, current efficiency is higher than fuel utilization.

For the above reasons, fuel utilization as defined in (7), not current efficiency, will be used in this work.

For the calculations of the efficiency and fuel utilization in this work, we use the lower heating value (LHV) of methane and other fuels (H_2 , CO), which is defined as the amount of heat produced by the complete combustion of a unit quantity of fuel when the water in the product is in a vapor form. This definition is consistent with the typical operating temperature of SC-SOFCs.

3. Computational setup

The numerical model used for this study has been applied in our previous studies for a spectrum of SC-SOFC performance and design problems [5,6]. The model involves modules that account for various physical and chemical processes critical for the fuel cell's performance, including flow convection and diffusion, heterogeneous chemistry, electrochemistry, mixed ionic–electronic conduction and heat transfer. For detailed model descriptions, the readers are referred to Ref. [6].

For the studies of efficiency and fuel utilization issues, an anode-supported yttria stabilized zirconia (YSZ) cell with nickel anode and $\text{Ba}_{0.5}\text{Sr}_{0.5}\text{Co}_{0.8}\text{Fe}_{0.2}\text{O}_{3-\delta}$ (BSCF) cathode used. The assumption of different materials of the electrodes goes with the heterogeneous reaction mechanisms of a CH_4 – O_2 mixture used by the numerical model for calculating the catalytic reactions in the anode and cathode, respectively. For microstructure parameters of the anode and cathode, the set of parameters in Ref. [5] is used. For electrochemistry and conductivity of the YSZ electrolyte, the set of parameters in Ref. [6] is used.

Compared with cells with mixed ionic–electronic conductor electrolytes (e.g. $\text{Ce}_{0.8}\text{Sm}_{0.2}\text{O}_{1.9}$ or SDC), the YSZ cell has the advantage of avoiding the reverse electronic current that could be extremely high at low oxygen contents, which keeps the computation from studying low oxygen flow rates because the total power

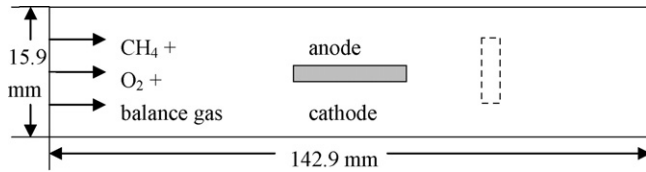


Fig. 1. The computation domain; the dashed line shows the possible layout of the cell.

output decreases much faster compared with YSZ cells. Thus, the YSZ cell is a better choice for studying the efficiencies in this work.

The computational setup is shown in Fig. 1. The dimensions of the gas chamber are 15.9 mm × 142.9 mm (height by length). One or more cells can be placed in the gas chamber, where in the case of one cell, the leading edge is 26.7 cm from the inlet. The thicknesses of the anode, electrolyte and cathode are 700, 15 and 10 μm, respectively. The length of the cell is 13.3 mm in the horizontal configuration and is divided into seven equal segments along its length direction. In the case of a perpendicular cell, the length will be redefined in the following discussion. The mixture of methane, oxygen and balance gas (nitrogen, helium or argon) is fed into the gas chamber from the inlet on the left, with the molar ratio of oxygen to balance gas fixed at 1:4. The operating temperature of the cell is 750 °C and load potential is 0.5 V unless stated otherwise.

4. Results and discussion

There are three major factors responsible for the low efficiency of SC-SOFCs: poor flow management, non-ideal electrode microstructure and low selectivity of the electrode materials. The materials side has been explored by many experimental groups by adopting novel electrodes [2] or improving traditional ones [12]. This work will focus on enhancing the efficiencies of SC-SOFCs by improving the flow management. The issue of the electrode microstructure will be discussed in our future work about SC-SOFC optimization.

By definitions (1) and (2), effective approaches that could improve the SC-SOFC efficiency and fuel utilization should enhance the electric power generation while keeping (or even reducing) the amount of fuel supply at the same time. With the fixed microstructure, catalytic properties and material properties of a given cell, the improvement of the power generation essentially amounts to optimizing the distribution of the reactants (i.e. both fuel and oxygen) around the cell, achievable through a careful management of the flow field in the gas chamber. In the following sections, flow management will be discussed in terms of fuel flow rate, fuel/oxygen ratio and flow geometry. The effect of using a cell stack is also discussed.

4.1. Fuel flow rate

Initially, a single cell placed horizontally in the gas chamber aligned with the centerline is simulated. The flow rate of CH₄ increases from 10 to 100 sccm (ml min⁻¹ at standard conditions) and the gas feed composition is fixed at CH₄:O₂:N₂ = 1:0.8:3.2. Consequently, the concentration of each incoming gas species is the same at all fuel flow rates, and so the influences of methane flow rate and total flow rate on the fuel cell's performance are equivalent.

The average power density and efficiencies are shown in Fig. 2, charted against the methane flow rate. In Fig. 2(a), when methane is less than 30 sccm, the power density increases almost linearly with methane flow rate, while the fuel cell efficiency stays above 7%. The fact that the efficiency is relatively constant in this region suggests that the electrical power generated by the fuel cell is transport-limited by the diffusion and convection of (some) gas species. When

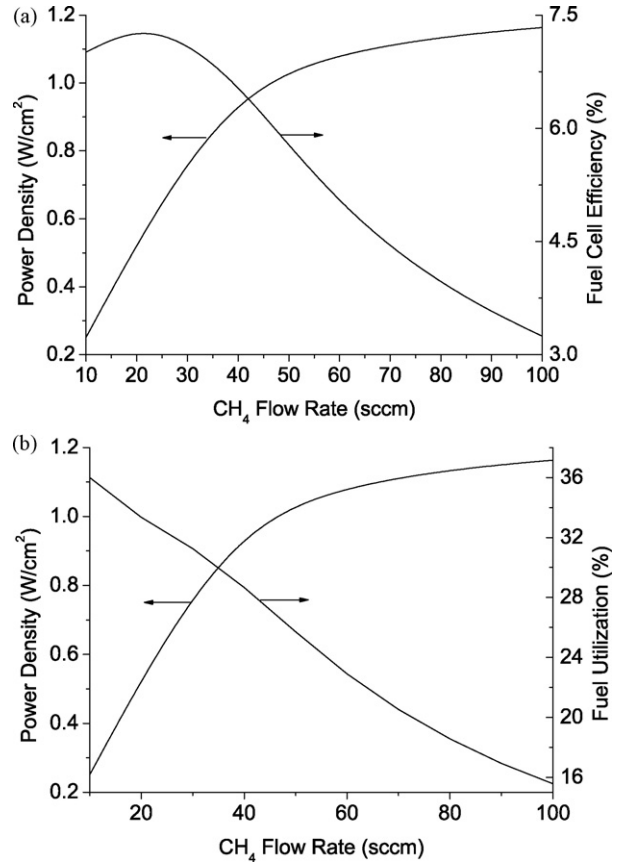


Fig. 2. Power density and efficiencies of a YSZ cell versus methane flow rate at CH₄:O₂:N₂ = 1:0.8:3.2, 750 °C and a load potential of 0.5 V; (a) efficiency and power density; (b) fuel utilization and power density.

methane is higher than 30 sccm, the power density gradually levels off and the efficiency decreases almost linearly to 3%, indicating that the transport limitation vanishes with high fuel flow rates. The argument for the transport limitation is supported by the distribution of power density along the cell, shown in Fig. 3. At low fuel flow rates, namely 30 sccm and below, the power density decays very sharply from the leading edge, so that the downstream portion of the cell does not make a significant contribution to the total power. This situation is greatly improved as the fuel flow rate increases beyond 40 sccm, for which the difference in local power density along the whole cell is small.

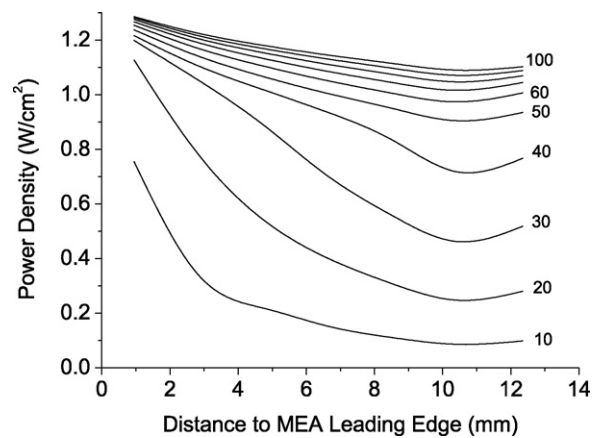


Fig. 3. Power density distribution along the cell at different methane flow rates with fixed flow rate ratio; methane flow rate (in sccm) is marked at the end of each curve.

The comparison between the curves with low and high fuel flow rates in Fig. 3 shows one evident difference that the former elevates almost universally and proportionally with the fuel flow rate regardless of location, while the latter shows only a relatively significant raise in power density at the downstream portion of the cell. This explains the different behaviors of the power density curve at different fuel flow rates shown in Fig. 2.

The influence of the flow rate on the power density, efficiency and fuel utilization of the fuel cell reveals the competition between the diffusion time scale and convection time scale of gases flowing around the cell. The diffusion time scale τ_{diff} , the average time it takes for a gas molecule to diffuse from the flow to the cell surface, can be estimated by the diffusion equation and half of the gap between the cell and the wall, i.e.

$$\tau_{\text{diff},k} = \frac{(h/4)^2}{D_k} \quad (11)$$

where h is the height of the channel and D_k is the diffusion coefficient of gas species k relative to the gas mixture. With the known gas composition above, the result is $\tau_{\text{diff},\text{CH}_4} = 7.8 \times 10^{-2}$ s and $\tau_{\text{diff},\text{O}_2} = 9.5 \times 10^{-2}$ s. Conversely, the convection time scale, the average time for a gas molecule to clear the cell length with the flow stream, can be calculated by the cell length L and the average flow speed \bar{v} over (or below) the cell, i.e.

$$\tau_{\text{conv}} = \frac{L}{\bar{v}} \quad (12)$$

With the flow geometry in Fig. 1 and the constant gas concentrations at the inlet, the diffusion time scale does not vary much. By comparison, the convection time scale is inversely proportional to the fuel flow rate. When the fuel flow rate is as low as 10 sccm, τ_{conv} is around 0.8 s, much longer than τ_{diff} . In this case methane and oxygen have sufficient time to diffuse to the cell to react, resulting in a relatively high efficiency and fuel utilization, but also leading to the significant depletion effect of the cell as shown in Fig. 3. Additionally, the proportional increase of local power density with flow rate in Fig. 3 explains the relatively constant fuel cell efficiency at low flow rates. However, when the fuel flow rate increases to 100 sccm, the convection time scale is reduced by a factor of 10 and is about the same as the diffusion time scale. As a result, a great portion of the fuel bypasses the cell unreacted, reducing the efficiency and fuel utilization. Understandably, the amount of unreacted fuel increases with the fuel flow rate, which accounts for the monotonic decrease of the efficiency curves at high flow rates in Fig. 2.

To have a better understanding of the fuel cell performance, Fig. 4 plots the conversion percentage of methane and oxygen versus methane flow rates. Compared to Fig. 2, the conversion curve of oxygen has a trend similar to the fuel cell efficiency curve, while the conversion curve of methane is very similar to the fuel utilization curve. This further indicates that for this case, the flow rate of oxygen is the controlling factor for the fuel cell efficiency at low flow rates, as oxygen has a higher conversion percentage than methane, and the transport limitation of oxygen is the bottleneck of the fuel cell efficiency.

The results above show that the fuel utilization of the SC-SOFC is low. Even at the lowest fuel flow rate, a major part of the fuel passes unreacted (esp. on the cathode side); increasing the flow rate generally leads to even lower efficiencies. The analysis about diffusion and convection time scales manifests the need for improving the flow management and geometric design of the gas chamber. Additionally, the result obtained under the fixed flow rate ratio indicates possible improvement by increasing the oxygen content. These points will be discussed as follows. Furthermore, out of the fuel utilized, only

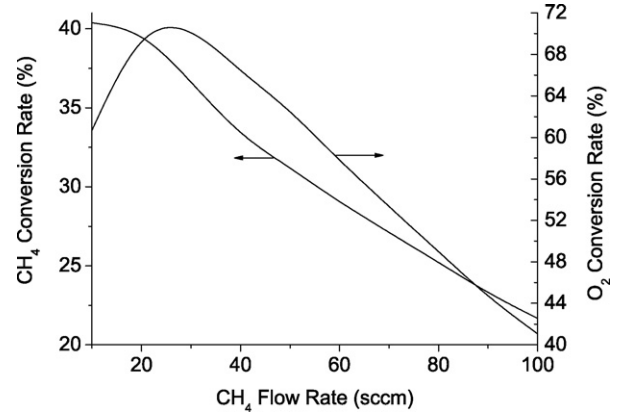


Fig. 4. Conversion percentage of methane and oxygen versus methane flow rate at $\text{CH}_4:\text{O}_2:\text{N}_2 = 1:0.8:3.2$.

about 20% is converted to electric power for all the flow rates calculated, meaning that a big part of the fuel is consumed by parasitic reactions on both electrodes. This requires further research for more selective electrodes and is beyond the scope of this paper.

4.2. Fuel/oxygen ratio

Based on the above analysis, the fuel cell efficiency could be improved by decreasing the fuel/oxygen ratio, especially for methane flow rates below 30 sccm. The improvement is demonstrated by simulation results at higher oxygen contents. Since the efficiency and fuel utilization are defined in terms of the fuel, it will be more convenient for the following discussions to use the oxygen/fuel ratio. Fig. 5 shows the fuel cell efficiency and fuel utilization for the $\text{O}_2:\text{CH}_4$ ratio increasing from 0.8 to 1.6 with a step size of 0.2, and the methane flow rate increases in the same way as above. Both figures show the same general trend, i.e. the efficiency and fuel utilization both decrease with the fuel flow rate (or equivalently the total flow rate). At the lowest methane flow rate, the (maximum) efficiency of each curve initially increases with the ratio up to 11.4% at $\text{O}_2:\text{CH}_4 = 1.2$, and then drops sharply afterwards, while the fuel utilization initially increases with the ratio and then stays almost constant. When methane flow rate is above 40 sccm, both the efficiency and fuel utilization decrease monotonically with the $\text{O}_2:\text{CH}_4$ ratio.

The change of the efficiency with respect to the $\text{O}_2:\text{CH}_4$ ratio is partly accounted for by the different behaviors of $i_{0,a}$ and $i_{0,c}$, the exchange current densities at the anode–electrolyte (A–E) and cathode–electrolyte (C–E) interfaces, defined as follows, respectively [6,13]:

$$i_{0,a} = i_{\text{H}_2}^* \frac{(p_{\text{H}_2,a}/p_{\text{H}_2}^*)^{1/4} (p_{\text{H}_2\text{O},a})^{3/4}}{1 + (p_{\text{H}_2,a}/p_{\text{H}_2}^*)^{1/2}} \quad (13)$$

$$i_{0,c} = i_{\text{O}_2}^* \frac{(p_{\text{O}_2,c}/p_{\text{O}_2}^*)^{1/4}}{1 + (p_{\text{O}_2,c}/p_{\text{O}_2}^*)^{1/2}} \quad (14)$$

where

$$p_{\text{O}_2}^* = A_{\text{O}_2} \exp\left(-\frac{E_{\text{O}_2}}{RT}\right), \quad p_{\text{H}_2}^* = \frac{A_{\text{des}} \Gamma^2 \sqrt{2\pi RT W_{\text{H}_2}}}{\gamma_0} \exp\left(-\frac{E_{\text{des}}}{RT}\right)$$

with $i_{\text{O}_2}^* = 2.8 \text{ A cm}^{-2}$, $A_{\text{O}_2} = 4.9 \times 10^8 \text{ atm}$, $E_{\text{O}_2} = 200 \text{ kJ mol}^{-1}$, $i_{\text{H}_2}^* = 8.5 \text{ A cm}^{-2}$, $\gamma_0 = 0.01$, $A_{\text{des}} = 5.59 \times 10^{19} \text{ s cm}^2 \text{ mol}^{-1}$, $\Gamma = 2.6 \times 10^{-9} \text{ mol cm}^{-2}$. The partial pressures of H_2 and H_2O at the

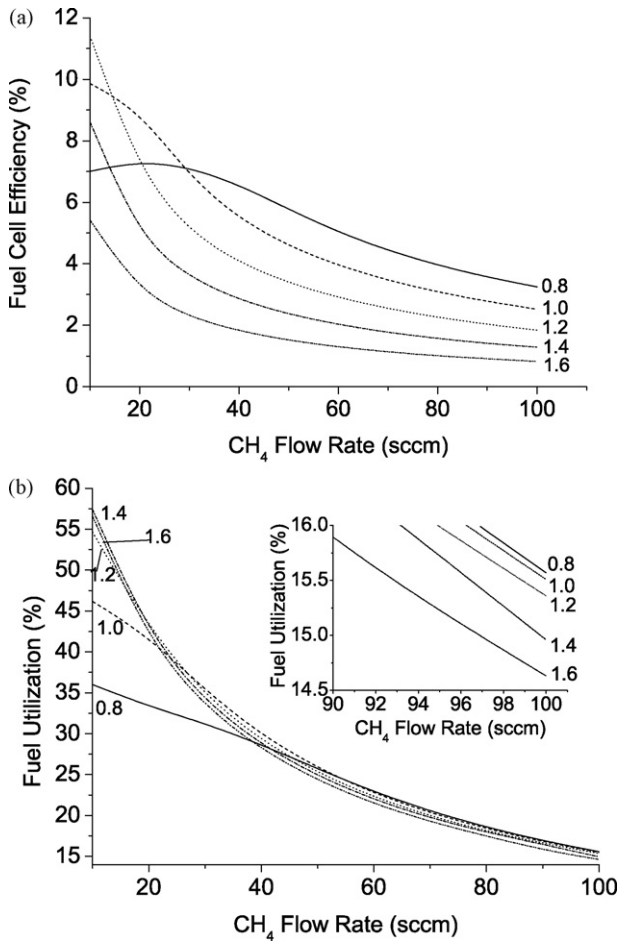


Fig. 5. Efficiency and fuel utilization of a YSZ cell at different O₂:CH₄ ratios (marked at the end or beginning of each curve); (a) fuel cell efficiency; (b) fuel utilization.

A–E interface, $p_{H_2,a}$ and $p_{H_2O,a}$, as well as the partial pressure of O₂ at the C–E interface, $p_{O_2,c}$, are all calculated by the numerical model.

Calculation shows that when the O₂:CH₄ ratio is below 1.2, $i_{0,c}$ is very sensitive to and increases with oxygen partial pressure $p_{O_2,c}$, which, in turn, increases significantly with the O₂:CH₄ ratio. For example, at a CH₄ flow rate of 10 sccm and a O₂:CH₄ ratio of 0.8, the O₂ partial pressure at the C–E interface varies from 2.9×10^{-8} to 1.7×10^{-4} atm along the length direction of the cell. The O₂ partial pressure increases to the range of 6.4×10^{-2} to 1.1×10^{-1} atm when the ratio increases to 1.6 with the same methane flow rate. As the O₂:CH₄ ratio increases beyond 1.2, $i_{0,c}$ saturates and becomes insensitive to $p_{O_2,c}$ (and consequently to the O₂:CH₄ ratio). Instead, $i_{0,a}$ decreases sensitively with the ratio and becomes dominant due to the saturation of $i_{0,c}$. Our results show that $i_{0,a}$ decreases because the global reaction in the anode becomes less favorable to H₂ production as the O₂:CH₄ ratio increases, reducing the H₂ concentration at the anode–electrolyte interface. The behaviors of $i_{0,a}$ and $i_{0,c}$ above is one possible reason for the monotonic decrease of fuel cell efficiency with the O₂:CH₄ ratio at high methane flow rates. Along the methane flow rate axis, when CH₄ is higher than 40 sccm, $i_{0,c}$ saturates due to the increase of $p_{O_2,c}$, and the fuel cell power output is predominantly determined by $i_{0,a}$, which decreases with the O₂:CH₄ ratio as the increasing concentration of oxygen reduces the production of hydrogen through the catalytic reactions over the Ni anode surface.

In particular, for methane flow rates above 40 sccm, which is typical in experimental literature, the efficiency monotonically

decreases with the O₂:CH₄ ratio. In relation to the behavior of the exchange current densities above, another possible reason for the drop of efficiency is the increase in the harmful oxidation of all possible fuels (methane, hydrogen and CO) with the rising oxygen content. This is illustrated by the ratio of the efficiency to fuel utilization, i.e. the portion of the fuel consumed that is converted to useful power, plotted in Fig. 6. It shows that the parasitic reactions on the electrode catalyst surfaces takes an increasingly higher portion of the total energy consumed, reinforcing the need for more selective electrode materials.

The influence of fuel/oxygen ratio on efficiency and fuel utilization is actually the combined effect of the electrochemical properties of the cell materials and the selectivity of the electrodes. High efficiencies are generally obtained at low flow rates, and the optimum fuel/oxygen ratio may shift when the flow rates are low, due to the depletion effect of either the fuel or the oxygen.

4.3. Flow geometry

As has been reported in literature, the layout of the cell in an SC-SOFC makes a difference in its performance [14]. The configuration with the cathode facing the fresh gas feed (i.e. cathode-first) yields a higher power density than the anode-first configuration. This is also verified by our previous work [5].

Here, we study the influence of the cell orientation on efficiency and fuel utilization. Compared with the last case, the cell is rotated so that it is perpendicular to the gas flow direction with the cathode facing the gas inlet, shown by the dashed line in Fig. 1. Limited by the vertical dimension of the gas chamber, the length of the cell is reduced to 5.3 mm. The flow rate combination of CH₄:O₂:N₂ = 100:120:480 sccm is used and all other conditions are the same as the previous case.

The result shows that the rotated cell generates a nearly uniform local power density of 0.72 W cm^{-2} along the length direction because any point on the cathode is exposed to the same gas mixture. The average power density is also higher than that of the horizontal case (0.66 W cm^{-2}). However, the total power is limited by the cell length and consequently, the efficiency and fuel utilization are only 0.8 and 12%, lower than their corresponding values of 1.8 and 15% of the horizontal case, respectively.

While it seems positive that increasing the cell length in the vertical direction will improve the total power and thus the efficiency, several disadvantages keeps this idea from being practical. First, with a given channel height, making the two ends of the cell

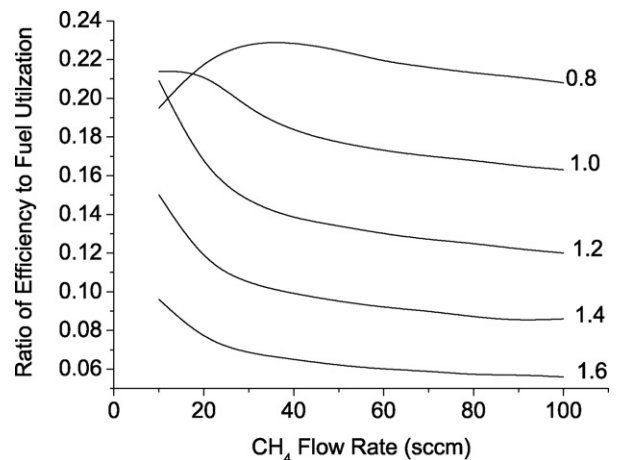


Fig. 6. The ratio of efficiency to fuel utilization for a YSZ cell; the corresponding O₂:CH₄ ratio is shown by each curve.

too close to the channel walls will greatly increase the upstream gas supply pressure and slow down the flow speed. The slow convection of the gas mixture will cause the oxygen near the cathode not to be replenished in time, making the electrochemical reaction of oxygen on the cathode side diffusion-limited and thus counteracting the advantage of the cathode-first configuration. Second, if the channel height is increased instead, the amount of unspent fuel will increase and the efficiencies will be reduced. Third, the vertical configuration would not work well in a stack. The primary reason for the single cell to generate a higher power density in this case is that the cathode-first flow geometry improves the oxygen partial pressure within the cathode, and by comparison, the anode-first configuration is worse because the oxygen partial pressure in the cathode is much lower [5]. So if one more vertical cell is put downstream (to make a stack), its performance will be seriously reduced due to the depletion of oxygen and fuel by the upstream one, no matter if it's anode-first or cathode-first.

Therefore, improving fuel cell performance by using vertical cells is not feasible, and we will continue to investigate other parameters for improving the efficiencies with the horizontal configuration.

4.4. SC-SOFC stack

The above analysis of the competition between diffusion and convection time scales demonstrates that the efficiencies of the SC-SOFC can be improved by reducing the length of the diffusion path of the gas reactant to the cell or increasing the length of the cell. One possible and straightforward approach might be using a narrower gas channel or a longer cell. However, it can be shown that when the flow speed of the gas mixture is the same, reducing the channel height would lead to a faster depletion of the fuel and oxygen along the cell, resulting in a lower power output. The idea of using a longer cell only slightly improves the efficiencies due to the depletion effect discussed in the first section.

Alternatively, the diffusion time scale can be effectively reduced by using an SC-SOFC stack with the cells being parallel to the flow direction with the same gas chamber dimensions and gas flow speed. For the simplicity of discussion, a two-cell stack in the anode-to-anode (a–a) configuration, similar to the one used by Shao et al. [2], will be examined. Compared with the single-cell case, the positions of the two cells are offset vertically and symmetrically from the channel centerline such that the distance between the two anodes is 0.60 cm. The incoming flow rates are set at $\text{CH}_4:\text{O}_2:\text{N}_2 = 100:80:320$ sccm. All other conditions are the same as before.

The computation results show that both the efficiency and fuel utilization are more than doubled compared with the single-cell case. The efficiency increases from 3.2 to 6.5%, and the fuel utilization increases from 15.6 to 37.3%. The reasons for the improvement, besides the shorter diffusion path of methane and oxygen to the cell, also include the following. First, the positions of the cells still leave a wide space between the two anodes and also between each cathode and its adjacent wall, replenishing the fuel and oxygen in a timely manner. Second, the anode-to-anode configuration reduces the amount of syngas (i.e. H_2 and CO) lost from the anodes to the gas flow outside the cell. Compared with the case of a single-cell, the gas mixture between the two anodes contains a higher concentration of syngas due to the symmetry, so that the spatial gradient of H_2 and CO at the anode–gas interfaces is reduced. Consequently, the concentrations of both H_2 and CO in the anode of the two cells are higher than in the single-cell case. This contributes to the improvement in power generation.

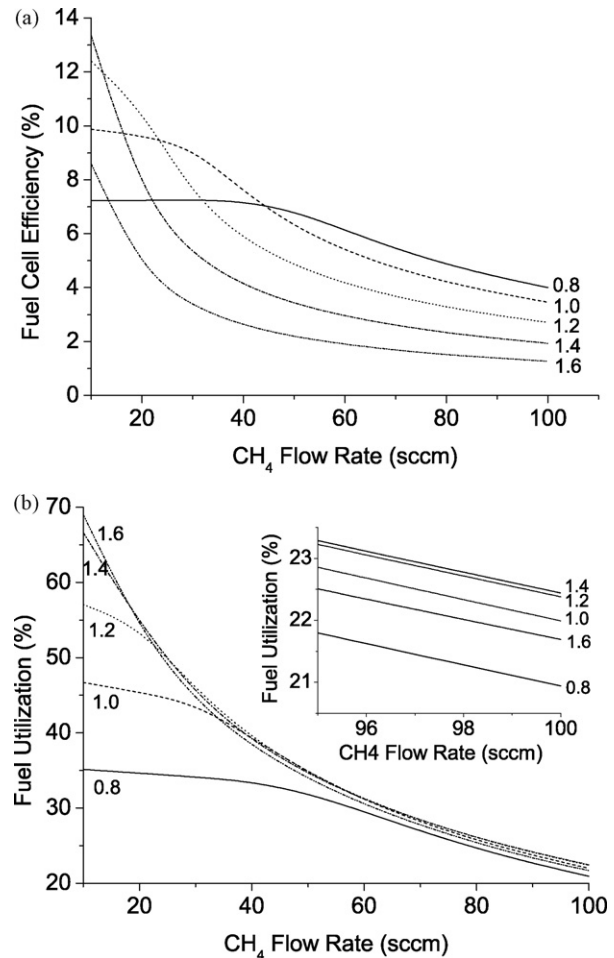


Fig. 7. Efficiency and fuel utilization of a YSZ cell with He balance gas at different $\text{O}_2:\text{CH}_4$ ratios (marked at the end or beginning of each curve); (a) fuel cell efficiency; (b) fuel utilization.

4.5. Balance gas

By definition (11), the diffusion time scale can also be reduced by increasing the diffusion coefficient D_k of gas species k . Since the balance gas takes up a major portion of the gas mixture, changing the balance gas should significantly affect the diffusion coefficient of each of the other species relative to the gas mixture and therefore affect the fuel cell efficiencies. For this purpose, the same cases discussed in the “fuel/oxygen ratio” section are computed with He being the balance gas, and the results are shown in Fig. 7.

The efficiency and fuel utilization curves exhibit a similar trend to the ones with N_2 balance gas. However, there are some important quantitative differences. First, both the efficiency and fuel utilization are higher than their corresponding values in the N_2 case (except very few points), with a difference of 0.5–5% for the former and 5–10% for the latter. Second, the highest efficiency is achieved at a higher fuel/oxygen rate (1.4) than that for N_2 (1.2).

To further explore the effect of the balance gas, the same computation was repeated with Ar balance gas, and the results are all very close to those of the N_2 . The difference between the SC-SOFC performances with He or Ar balance gas indicates that He helps to improve the diffusion coefficient of both methane and oxygen, which leads to noticeable changes of the gas transport between the gas mixture and the cell, while on the other hand, the changes brought by Ar is minimal. This is verified by the comparison of diffusion coefficients of all gas phase species relative to the gas mixture

Table 1
Diffusion coefficients of gas species with different balance gases; unit: $\text{m}^2 \text{s}^{-1}$

	N_2	He	Ar
CH_4	2.03×10^{-4}	3.44×10^{-4}	2.08×10^{-4}
H_2	6.06×10^{-4}	8.89×10^{-4}	6.27×10^{-4}
CO	1.70×10^{-4}	3.10×10^{-4}	1.67×10^{-4}
O_2	1.66×10^{-4}	2.42×10^{-4}	1.71×10^{-4}
CO_2	1.38×10^{-4}	2.60×10^{-4}	1.34×10^{-4}
H_2O	2.19×10^{-4}	3.98×10^{-4}	2.20×10^{-4}
B.G. ^a	1.56×10^{-4}	1.17×10^{-3}	1.19×10^{-4}

^a B.G. is the balance gas, e.g. for the “ N_2 ” column, it means N_2 , etc.

with one of the three balance gases in Table 1. The calculation is performed by CANTERA [15] for a typical gas mixture composition of $\text{CH}_4:\text{O}_2:\text{B.G.} = 1:0.8:3.2$, where B.G. means the balance gas.

5. Conclusions

The efficiencies of the single-chamber SOFCs are generally low. Many of the reasons that account for the low efficiencies trace back to the mixing of fuel and oxygen and the one-gas-chamber geometry, which are inherent in the definition of this type of fuel cell. However, the fuel cell efficiencies can be effectively improved through flow management. Through the numerical study of a YSZ cell running on the mixture of methane and air, this work systematically investigates the influence of many operating parameters, primarily concerning the flow field in the gas chamber, on the efficiency and fuel utilization of the fuel cell, and demonstrates approaches for improving the fuel cell performance.

Compared with the dual-chamber SOFCs, the cell length of an SC-SOFC is much shorter than that of the gas chamber, so that the convection time scale of the flow over the cell is significantly reduced. Consequently, the fuel and oxygen in the gas mixture may not have sufficient time to diffuse to the electrodes of the cell for subsequent reactions, and therefore the efficiencies of the SC-SOFC is to a large extent determined by the competition between the diffusion time scale and the convection time scale. For SC-SOFCs with a single cell, when the time scale of convection is much longer than that of diffusion (e.g. long cell or slow flow speed), high efficiency and fuel utilization can be achieved, but the depletion of fuel and oxygen by the upstream portion of the cell is also serious, resulting in a low total power; when the time scale of diffusion is much longer than that of convection (e.g. wide gas chamber or fast flow speed), the local power density at the downstream part of the cell increases significantly and the total power is boosted, but the amount of the unspent fuel also increases proportionally with the flow speed, resulting in a low efficiency and fuel utilization.

The simulation results show that for single-cell SC-SOFCs high efficiencies and high power are not likely to be achieved at the same time. However, this seeming contradiction can be mitigated by using a two-cell stack, which effectively reduces the diffusion time scale while still allowing enough gas supply for both electrodes. Also, operating the fuel cell under optimum fuel/oxygen ratio and with highly diffusive balance gas both help to improve the efficiencies. Other approaches, including rotating the cell, reducing the gas chamber width, or increasing the length of the single cell are found not as effective.

Although the efficiencies at low fuel flow rates (< 30 sccm) are high, such flow rates are less desirable for practical applications and are rarely used in experimental literature, because the electric power is limited by the low energy flux of the fuel. On the other hand, too high of a fuel flow rate (> 100 sccm) is also undesirable because it does not bring significant benefits to the total power but rather greatly increases the amount of unspent fuel. Many experimental studies used fuel flow rates between 30 and 100 sccm with comparable gas chamber dimension [12,16].

While at high fuel flow rates the major barrier to high efficiencies is the unreacted fuel, at low flow rates the major obstacle is the parasitic reaction over the electrode catalyst surfaces. The simulation results show that the fuel utilization can be as high as 67% (with He balance gas at the lowest fuel flow rate), but only one-fifth of the consumed fuel is converted to useful power. This presents a major challenge to the research for more selective electrode materials.

The simulation also shows that in the frequently used fuel flow rate range, the achievable efficiency can be considerably higher than what's reported in experimental literature ($\sim 1\%$). In reality, high efficiencies could be achieved by the optimization of flow rate control and would be further improved by the adoption of cell stacks as well as future advances in materials science, which will make the application of SC-SOFCs for real portable power generation needs highly possible.

Acknowledgments

This work was partly supported by the Defense Advanced Research Projects Agency (DARPA) under grant N66001-01-1-8966 and partly by the Office of Naval Research under grant N00014-05-1-0339. We greatly appreciate the constructive suggestions from S. M. Haile, Z. Shao, C. Pantano, W. Lai, J. Mederos and Vaughan Thomas.

References

- [1] M. Yano, A. Tomita, M. Sano, T. Hibino, *Solid State Ionics* 177 (2007) 3351.
- [2] Z.P. Shao, S.M. Haile, J. Ahn, P.D. Ronney, Z.L. Zhan, S.A. Barnett, *Nature* 435 (2005) 795.
- [3] T.W. Napporn, X. Jacques-Bedard, F. Morin, M. Meunier, *J. Electrochem. Soc.* 151 (2004) A2088.
- [4] T. Hibino, A. Hashimoto, T. Inoue, J. Tokuno, S. Yoshida, M. Sano, *J. Electrochem. Soc.* 147 (2000) 2888.
- [5] Y. Hao, Z.P. Shao, J. Mederos, W. Lai, D.G. Goodwin, S.M. Haile, *Solid State Ionics* 177 (2006) 2013.
- [6] Y. Hao, D.G. Goodwin, *J. Electrochem. Soc.* 154 (2007) B207.
- [7] H.Y. Zhu, R.J. Kee, *J. Electrochem. Soc.* 161 (2006) 957.
- [8] T. Suzuki, P. Jasinski, V. Petrovsky, H.U. Anderson, F. Dogan, *J. Electrochem. Soc.* 151 (2004) A1473.
- [9] T. Suzuki, P. Jasinski, V. Petrovsky, H.U. Anderson, F. Dogan, *J. Electrochem. Soc.* 152 (2005) A527.
- [10] N.Q. Minh, T. Takahashi, *Science and Technology of Ceramic Fuel Cells*, Elsevier, New York, 1995, p. 24.
- [11] Y. Hao, D.G. Goodwin, *J. Electrochem. Soc.* 155 (2008) B666.
- [12] T. Hibino, A. Hashimoto, M. Yano, M. Suzuki, S. Yoshida, M. Sano, *J. Electrochem. Soc.* 149 (2002) A133.
- [13] H.Y. Zhu, R.J. Kee, V.M. Janardhanan, O. Deutschmann, D.G. Goodwin, *J. Electrochem. Soc.* 152 (2005) A2427.
- [14] I.C. Stefan, C.P. Jacobson, S.J. Visco, L.C. De Jonghe, *Electrochem. Solid State Lett.* 7 (2004) A198.
- [15] D.G. Goodwin, *Chemical Vapor Deposition XVI and EUROCVD 14*, *Electrochem. Soc.*, 2003, p. 155.
- [16] Z.P. Shao, J. Mederos, W.C. Chueh, S.M. Haile, *J. Power Sources* 162 (2006) 589.